Characteristics of Landslide Distribution and Dimension, Comparison of Landslides Induced by Reverse-fault Earthquake and Normal-fault Earthquake in Japan

Baator HAS,[1*] Toko TAKAYAMA[1], Satoshi ONODA[1] and Kiichiro OGAWA[1]

[1] Asia Air Survey, Co., Ltd. (1-2-2 Manpukuji, Asao-ku, Kawasaki, Kanagawa 1150004, Japan)
*Corresponding author. E-mail: has.baator@ajiko.co.jp

In this paper, to clarify the characteristics of landslides induced by reverse-fault and normal-fault earthquakes, distribution and scale of landslides induced by the Iwate-Miyagi earthquake in 2008 and Fukushima Hamadori earthquake in 2011 were analyzed. The results showed that in the both cases, the landslides were mostly distributed on the hanging wall of the source fault and the size of landslides was likely to be larger than that on the foot wall. However, the number of landslides induced by normal-fault earthquake is significantly fewer than that induced by reverse-fault earthquake and the size of landslides tends to be smaller than that of induced by reverse-fault earthquake. These characteristics coincide with the peak ground acceleration distribution of different type earthquakes, considered to be related with the hanging wall effect of reverse-fault and normal-fault earthquakes.

Key words: earthquake-induced landslide, reverse fault, normal fault, peak ground acceleration

1. INTRODUCTION

After 2004, a series of strong earthquakes struck eastern Japan, caused severe damage to the focal areas. In the cases of earthquakes occurred in mountainous areas, most of the victims were always caused by earthquake-induced landslides and debris flows [e.g. Ushiyama and Ohta, 2009]. The issue of earthquake-induced landslides has been a significant problem related to reduce victims of earthquake disasters.

Different fault type earthquakes may induce different characterized landslides, especially related to their distribution and dimension. In the inland of eastern Japan, because of the east-west compression caused by the Pacific Ocean plate subducting under the Eurasian plate [*Taira, 2001*], evidently earthquakes are expected to be initiated by reverse faults. Recent strong earthquakes, such as the Chuetsu earthquake in 2004, the Chuetsu-oki earthquake in 2007 and the Iwate-Miyagi Inland earthquake in 2008, all occurred on reverse faults, demonstrated the east-west compression in the eastern Japan. These reverse-fault earthquakes involved in mountainous areas, caused a large number of landslides [*e.g. Chigira and Yagi, 2005; Hasegawa et al., 2009; Yagi et al*, 2008]. Regarding normal-fault earthquake-induced landslides, there was no well documented example because normal-fault earthquake is not a common phenomenon in Japan, especially in eastern Japan which is under the east-west compression stress. However, Fukushima Hamadori earthquake occurred in Fukushima prefecture just one month after the great Tohoku earthquake in 2011 [*JMA, Japan Meteorological Agency, 2011*] was a rare case of normal-fault strong earthquake in eastern Japan. It provided us an opportunity to study normal-fault earthquake-induced landslides.

In this paper, to clarify the differences between landslides induced by reverse-fault and normal-fault earthquakes, two recent earthquakes are analyzed. One is the Iwate-Miyagi Inland earthquake (hereafter Iwate-Miyagi earthquake) occurred in 2008, which marked M_{JMA}7.2 and intensity of 6 *upper* in JMA scale. And another is the Fukushima Hamadori (hereafter Fukushima) earthquake occurred in 2011, marked M_{JMA}7.0 and intensity of 6 *lower* in JMA scale [*JMA, 2011*]. The parameters of the two earthquakes are listed in the **Table 1**.

In this study, the landslides induced by earthquakes were extracted from aerial photographs and the satellite images of Google Earth. The distance from source fault was calculated as the

shortest distance between the central point of landslide and surface projection of source fault. The source faults were referred to *Hikima et al*., [*2008*] for the Iwate-Miyagi earthquake and *GSI* [*2011*] for the Fukushima earthquake, respectively. Since the Fukushima earthquake occurred on a complex fault system [*Hikima, 2012; Fukushima et al., 2013*], considering the south western dip of these normal faults, the eastern most Yunotake fault (see **Fig.2b**) was selected as the source fault to calculate the distance from landslide to source fault.

Table 1 Parameters of the two earthquakes involved in this study

Name of Earthquake	Date (Local)	Epicenter		M (JMA)	Depth (km)	Source Fault			Max Intensity (JMA)	PGA (gal)
		Lat.	Long.			Strike	Dip	Type		
Iwate-Miyagi	Jun.14, 2008	39°01.7′	140°52.8′	7.2	8	N21E-N11E	41NW	Reverse	6 *upper*	4022.1
Fukushima	Apr.12, 2011	36°54.7′	140°40.3′	7.0	6	N50W	SW	Normal	6 *lower*	745.8

2. REGIONAL SETTINGS

Study areas are shown in **Fig. 1**. The study area 1 is located in the north eastern Japan, where distances about 370 km north east from Tokyo. The study area 1, occupies about 1,042 km^2, is around the source fault and focal area of the Iwate-Miyagi earthquake (see **Fig. 2a**).

The Study area 2 is also located in north eastern Japan and distances about 170 km north east from Tokyo. The study areas 2 occupies about 720 km^2, is around the source fault and the focal area of the Fukushima earthquake (see **Fig.2b**).

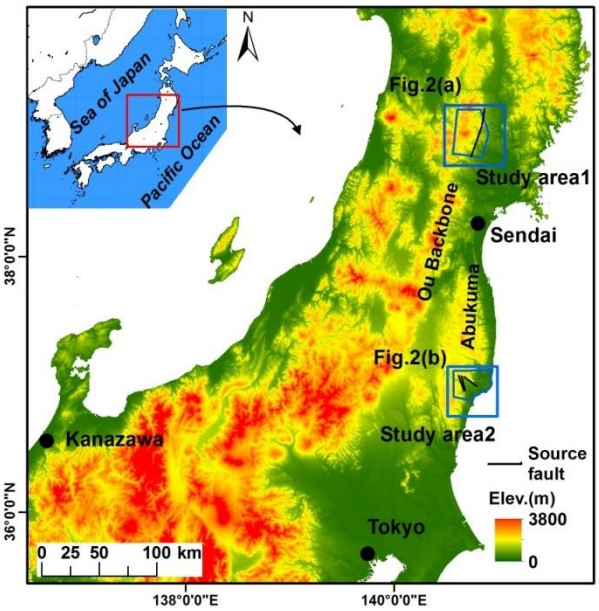

Fig. 1 Location map of study areas.
Background is made from ASTER GDEM (Product of Ministry of Economy, Trade, and Industry (METI) of Japan and the United States National Aeronautics and Space Administration (NASA)).

The Iwate-Miyagi earthquake occurred on northwest dipping reverse fault [*Hikima, 2008*], while the Fukushima earthquake occurred on southwest dipping normal faults [*Hikima, 2012; Fukushima et al., 2013*] (**Table 1**).

2.1 Topographic setting

The study area 1 and its vicinities are included in the central part of the Ou Backbone range (**Fig. 1**). The elevation of hills and mountains in the study area ranges from about 300 to 1,600 m above sea level (**Fig. 2a**). The mountainous area was eroded by rivers and formed steep slopes. The study area 2 is located in the central to southern part of the Abukuma highland (**Fig. 1**). The hills, ranges from about 100 m to 800 m above sea level (**Fig. 2b**), are characterized by gentle slopes. Hills in the study area 2 are gentler than that in study area 1.

Fig. 3 shows slope angle distribution of the study areas and their surroundings. The slope angle is calculated from ASTER GDEM and the mesh size is 30 x 30 m. The study area 1 includes large number of steep slope meshes compared to that in the study area 2 (**Fig.4**).

2.2 Geological setting

Fig. 5 shows geological maps of the study areas. In the study area 1, the geology is mostly composed of volcanic rocks from Neogene to Quaternary. Sedimentary rocks of Neogene to Quaternary also occupy a small percent of the region. Compared to the study area 1, the study area 2 is mostly occupied by plutonic rocks and metamorphic rocks (Cretaceous) in the mountainous area. However, in the gentle hills, the geology is mostly composed of sedimentary rocks from Neogene to Quaternary.

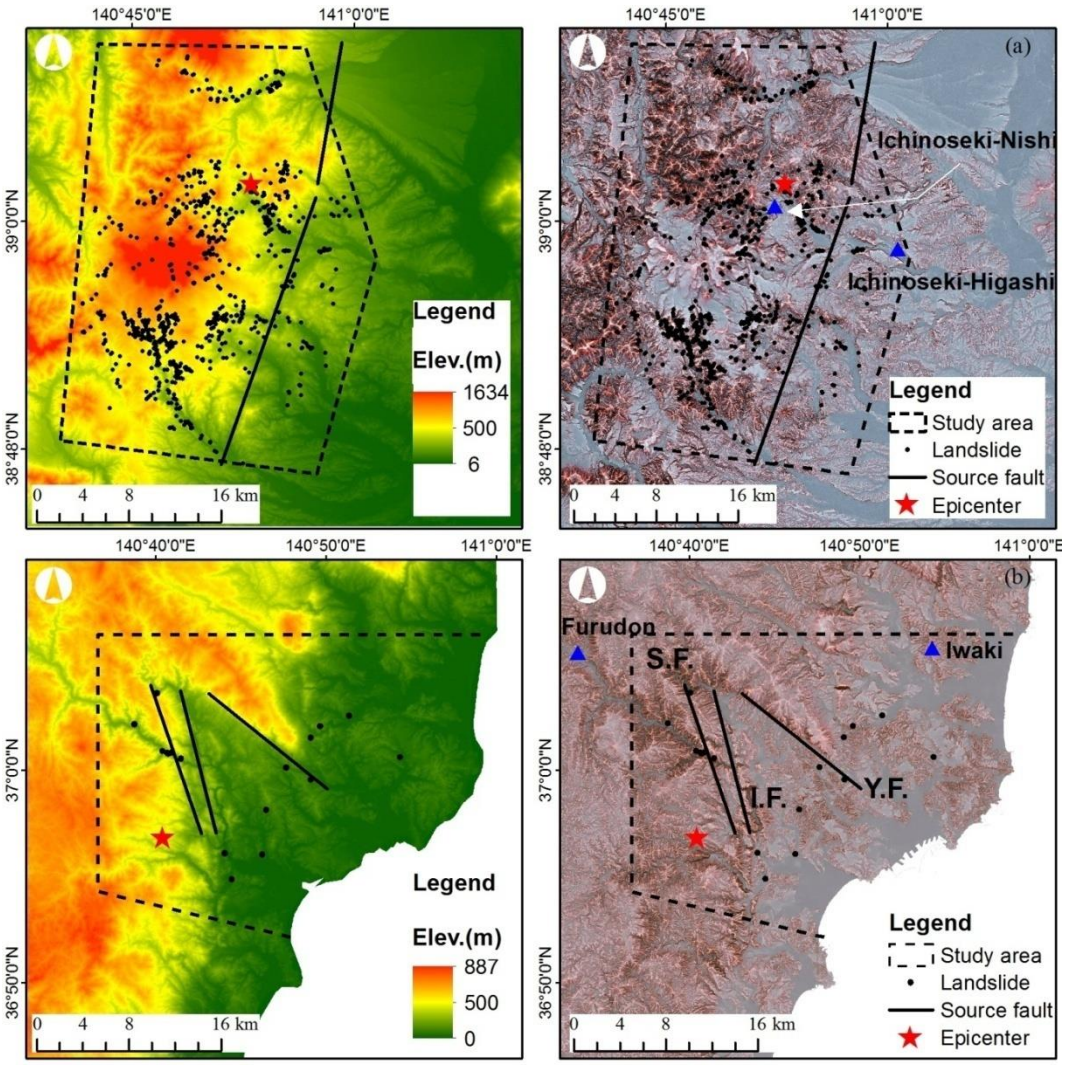

Fig.2 Elevation map (left) and red relief image map [right, *Chiba et al.*, 2008] of the study areas.
(a) Study area 1 (Iwate-Miyagi earthquake); (b) Study area 2 (Fukushima earthquake). Inside, black solid lines indicate, S.F: Shiodaira fault; I.F.: Idosawa fault; Y.F.: Yunotake fault. The distance from source fault to landslide refers to the Yunotake fault. Elevation map is made from ASTER GDEM 30 m mesh data (product of METI and NASA).

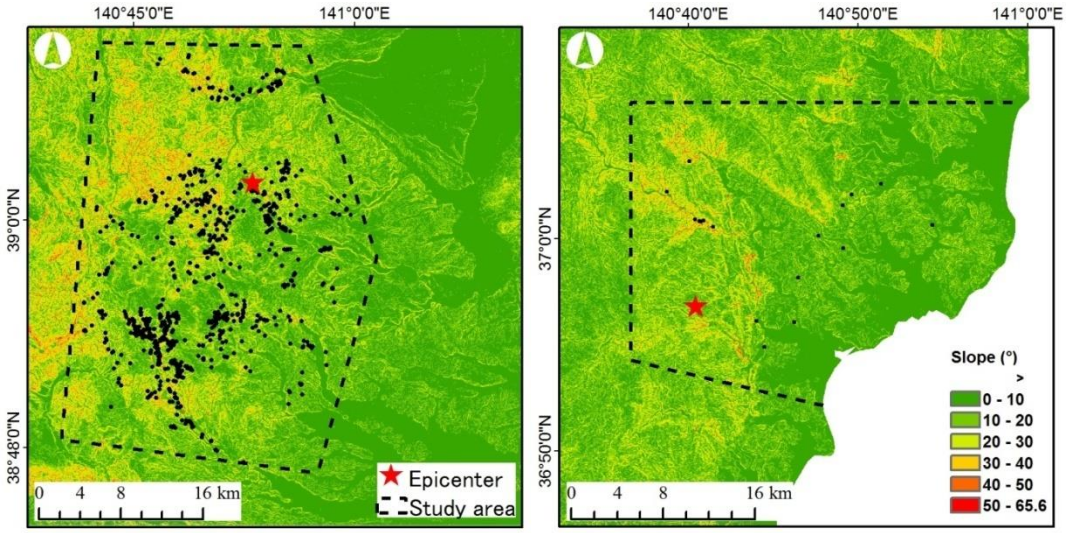

Fig.3 Slope angle of study areas
Left: Iwate-Miyagi earthquake; Right: Fukushima earthquake.
The slope angle is calculated from 30 m mesh ASTER GDEM.

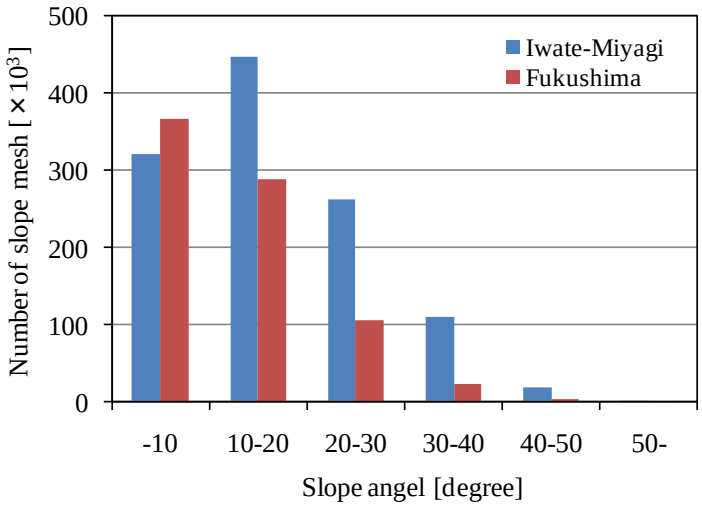

Fig. 4, Distribution of slope angle mesh (30x30 m) in the study areas.

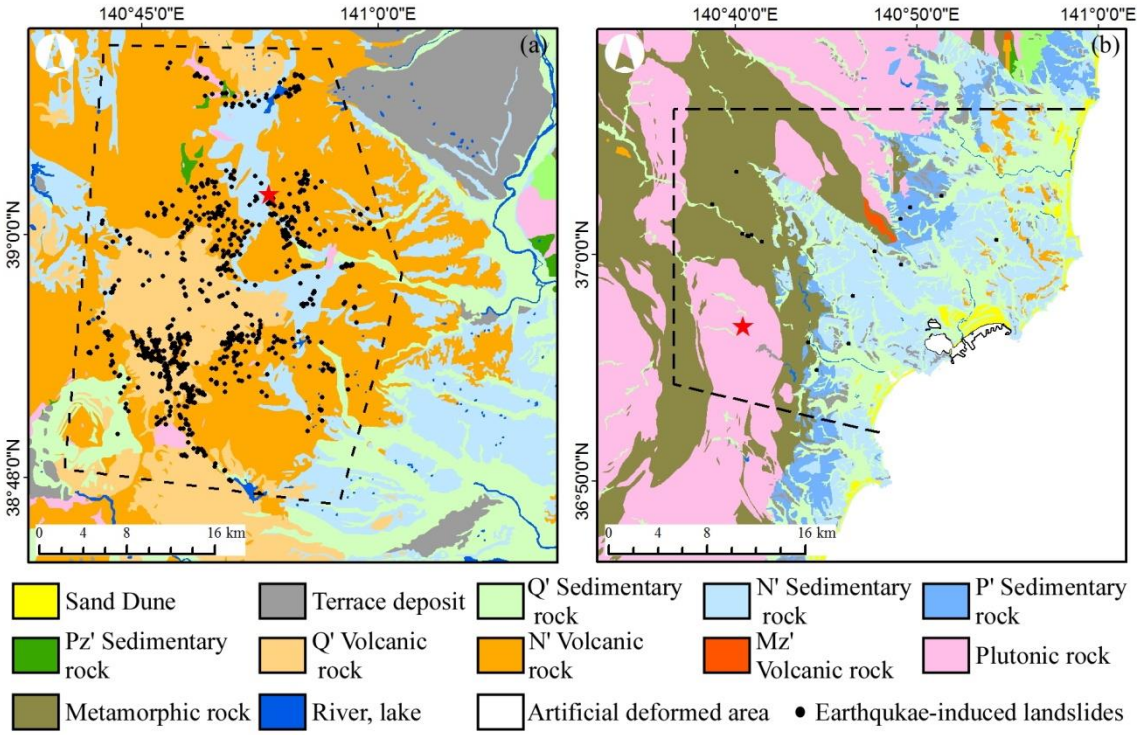

Fig. 5 Geological map of the study areas. Data from digital geological map of *Geological Survey of Japan* [2012].
(a) Iwate-Miyagi earthquake; (b) Fukushima earthquake
In legend, Q: Quaternary; N: Neogene; P: Paleogene; Mz: Mesozoic; Pz: Paleozoic.

Table 2 Inventory of earthquake-induced landslides

Name of Earthquake	Area (km^2)	Landslides				
		Total number	Hanging wall (number / %)		Foot wall (number / %)	
Iwate-Miyagi	1042	810	741	91.5	69	8.5
Fukushima	720	17	13	80.0	4	20.0

3. CHARACTERISTICS OF EARTHQUAKE-INDUCED LANDSLIDES

The landslide induced by the two earthquakes were extracted from aerial photographs and the satellite images of Google Earth. The landslides inventory data are shown in **Table 2**. For these landslides, the characteristics of distribution as well as the dimensions with the distance from source fault were analyzed. Landslides distribution with the Peak Ground Acceleration (PGA) was also analyzed.

3.1 Spatial distribution of landslides

For both earthquakes, more than 80% of the landslides occurred on the hanging wall sides, although the numbers of landslides showed far different characteristic between them (**Table 2, Fig. 2**). Compared to the Fukushima earthquake, the Iwate-Miyagi earthquake induced about 48 times more number of landslides.

3.2 Landslides number and dimension with distance from source fault

Fig. 6 shows the relationship between the landslide size (area) and the distance from the source faults. The landslides induced by the Iwate-Miyagi earthquake distributed within 20 km from the source fault. Compared to the Iwate-Miyagi earthquake, the landslides induced by the Fukushima earthquake distributed only within about 7 km from the source fault. In the case of the Iwate-Miyagi earthquake, the landslides occurred in a larger area far from the source fault than that of the case of the Fukushima earthquake (**Fig. 2**). The results showed that compared to normal-fault earthquake, reverse-fault earthquake tends to induce landslides in a wider area far from source faults.

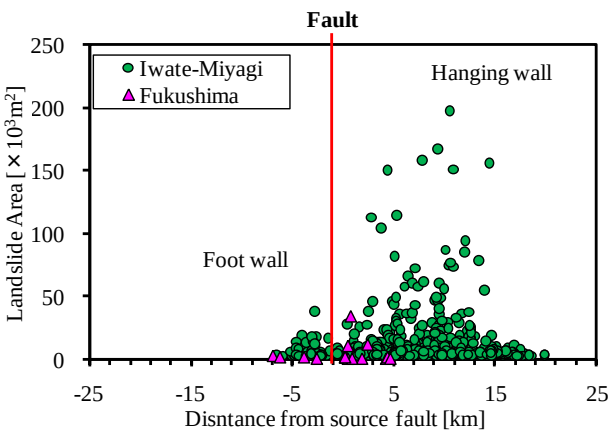

Fig. 6 Landslide size with distance from source fault

For both the reverse-fault and normal-fault earthquakes, the maximum size of landslides distributed on hanging wall sides was larger than that on the footwall. On the hanging wall, the largest landslide induced by the Iwate-Miyagi earthquake was about 2,000,000 m^2 while the largest one induced by the Fukushima earthquake was about 34,000 m^2. Compared to the normal-fault earthquake, the reverse-fault earthquake tends to induce large-scale landslides.

Fig.7 shows the landslides frequency distribution with distance from the source faults. In the case of the Iwate-Miyagi earthquake, about 84% of the landslides occurred within 12 km from the source fault, and the number of landslides decreases with the distance increasing. For the Fukushima earthquake, more than half of total landslides occurred within 2 km from the source fault and the number decreases with distance increasing.

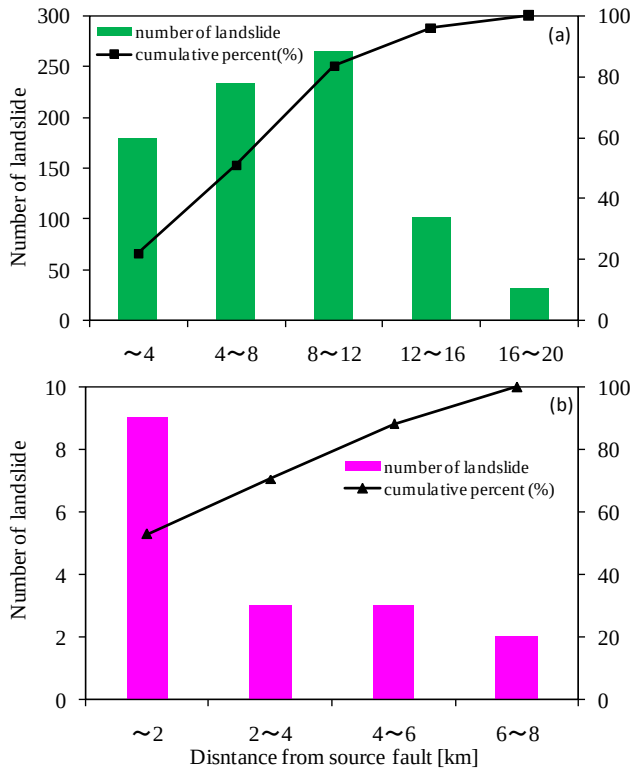

Fig. 7 Landslide frequency distributions with distance from source fault.
(a) Iwate-Miyagi earthquake; (b) Fukushima earthquake

4. DISCUSSION

According to above results, landslides distribution shows similar characteristics in both reverse-fault and normal-fault type earthquakes. In both cases, most of the landslides occurred on the

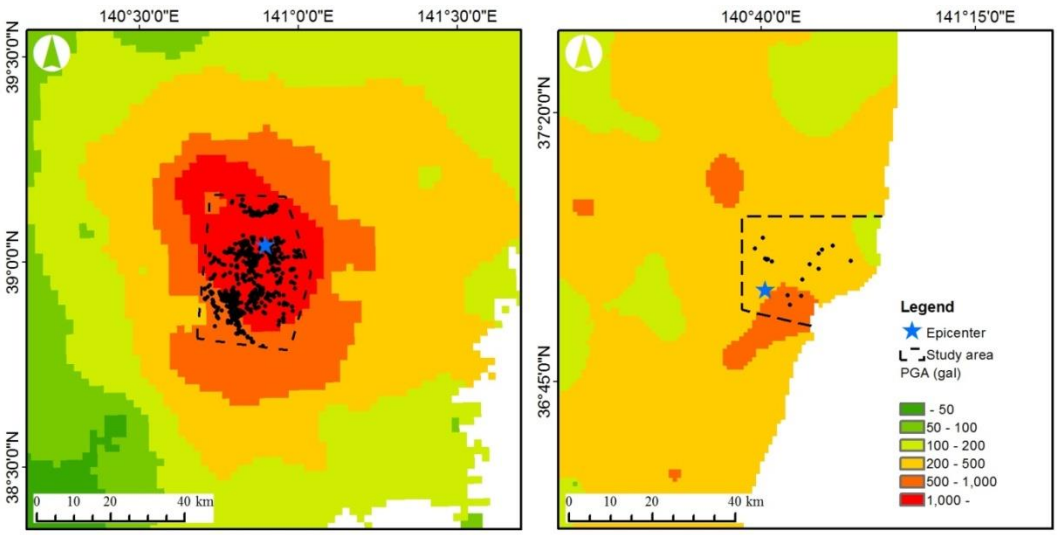

Fig. 8 Landslides distribution with PGA
Left: Iwate-Miyagi earthquake; Right: Fukushima earthquake
The distribution map was drawn by GIS function using unified PGA data from NIED [2014]

hanging wall sides of the source faults. This characteristic was considered to be related to the PGA distribution feature of inland earthquakes known as the hanging wall effects [e.g. *Abrahamson and Somerville, 1996; Shi et al., 2003*; *Chang et al*., 2004]. However, in this study, the reverse-fault earthquake induced a large number of landslides, including large-scale ones compared to that of normal-fault earthquake. Also, compared to the normal-fault earthquake, the reverse-fault earthquake induced landslides in a longer distance from the source fault. These characteristics coincide with the difference of PGA distribution between reverse-fault and normal-fault earthquakes. Usually, in cases of similar magnitude earthquakes, the PGA of reverse fault earthquake is larger than that of normal-fault earthquake [*McGarr, 1984; Abrahamson and Shedlock, 1997; Oglesby et al., 1998*].

Fig. 8 shows the PGA distributions of the two earthquakes. In the case of the Iwate-Miyagi earthquake, the PGA in and around the study area was predominantly larger than that in the case of the Fukushima earthquake. The study area 1 was mostly occupied by zones of PGA larger than 500 gal. This feature shows similar tendency of other reverse-fault earthquake-induced landslides [*Hasi et al.,* 2011]. However, in the case of the Fukushima earthquake, the area indicating PGA more than 500 gal was limited and only few landslides were triggered. Therefore, the number of landslides induced by the case of the Iwate-Miyagi earthquake is predominantly larger than that by the Fukushima earthquake coincide with the characteristics of the PGA distribution of the two earthquakes. The results show that the PGA distribution play strong influence to landslides occurrence.

Fig. 9 shows particle motion of seismic waves from stations on hanging wall and footwall of the source fault (see **Fig.2**). In both cases, the PGA on the hanging wall sides is larger than that on the foot wall sides. Also, compared to reverse-fault earthquake, normal-fault earthquake induced PGA is much smaller. This fact indicates that ground motion of the two earthquakes is much different even though with similar magnitude.

However, local geological, geomorphological and meteorological conditions may influence the landslide occurrence by strong earthquakes. In this study, the geological components are different in two study areas. The study area 1 is predominantly occupied by volcanic rocks, but the study area 2 is mostly occupied by plutonic and metamorphic rocks in mountainous area. This different local geological distribution more or less influenced the landslide occurrence, but significant differences that role the occurrence of landslides is still unknown. Also, compared to the study area 2, the steeper slopes in study area 1 more or less influenced landslides occurrence. Future works are necessary for revealing the effects of local geological and geomorphological conditions on landslides occurrence by strong different fault type earthquakes.

About strike-slip fault earthquakes in the inland Japan, like the Kobe earthquake (M7.3, 1995) and the Western Tottori earthquake (M7.3, 2000), compared to reverse-fault earthquakes, induced very few or no large-scale landslides [*Kubota*, 2002], or the slope failures were usually very shallow

[*Tainosho and Fujita*, 1996]. These characteristics suggest that different type earthquakes may induce different distribution and size of landslides.

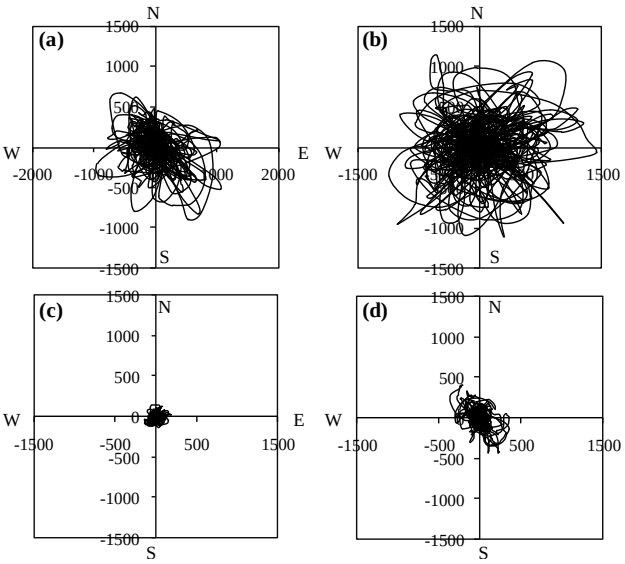

Fig. 9 Particle motion of the PGA from stations on footwall (a, c) and hanging wall (b, d) of KiK-net and K-NET of NIED [2014]. Unit is gal.
(a) Ichinoseki-Nishi, (b) Ichinoseki-Higashi (Iwate-Miyagi earthquake, see **Fig. 2a**); (c) Furudon, (d) Iwaki (Fukushima earthquake, see **Fig. 2b**).

5. CONCLUSION

This paper compared the characteristics of landslides induced by two different type strong earthquakes, reverse-fault one represented by the Iwate-Miyagi inland earthquake and normal-fault one represented by the Fukushima earthquake occurred in eastern Japan. The results showed that there are some similarities and differences between reverse-fault and normal-fault earthquake-induced landslides in their distribution and size. For both reverse-fault and normal-fault earthquakes, most of the landslides occurred on hanging wall sides, and the size of landslides tend to be larger on the hanging wall than that on the footwall. However, compared to reverse-fault earthquake, normal-fault earthquake tends to induce fewer and smaller landslides. Without considering local geological and geomorphological conditions, all these characteristics seemed to be related with the PGA distribution features of vertical fault earthquakes.

The results suggested that the different fault-type inland earthquakes are possible to induce different characterized landslides under a similar earthquake magnitude. Future work is necessary for reveal the details of characteristics of landslides induced by different fault-type earthquakes, including strike-slip fault earthquake.

ACKNOWLEDGEMENT: The authors are grateful to Dr. Daimaru and two anonymous reviewers, for their constructive comments.

REFERENCES

Abrahamson, N. A. and K. M. Shedlock (1997). Overview, Seism. Res. Lett. Vol. 68, pp.9–23.

Abrahamson, N. A. and Somerville, P. G. (1996): Effects of the hanging-wall and footwall on ground motions recorded during the Northridge earthquake, Bull. Seimo. Soci. America, Vol. 86, No.1B, pp.S93-99.

Chang, T. Y., Cotton, F., Tsai, Y. B. and Angelier, J. (2004): Quantification of hanging-wall effects on ground motion :some insights from the 1999 Chi-Chi earthquake, Bull. Seis. Soc. of America. Vol. 94, No. 6, pp. 2186-2197.

Chiba, T., Kaneta, S. and Suzuki, Y. (2008): Red Relief Image Map: New visualization method for three dimensional data, The International Archives of the Photogrammetry, Remote Sensing and Spatial Information Sciences, Vol. XXXVII, pp. 1071-1076.

Chigira, M. and Yagi, H. (2005): Geological and geomorphological characteristics of landslides triggered by the 2004 Mid Niigata prefecture earthquake in Japan. Engineering Geology. Vol. 82, pp. 202–221.

Fukushima, Y., Takada, Y. and Hashimoto, M. (2013): Complex Ruptures of the 11 April 2011 Mw 6.6 Iwaki Earthquake Triggered by the 11 March 2011 Mw 9.0 Tohoku Earthquake, Japan, Bull. Seismol. Soc. Am., Vol.103, pp.1572-1583, doi: 10.1785/0120120140.

Geological Survey of Japan (2012): AIST (ed.), Seamless digital geological map of Japan 1: 200,000. Jul 3, 2012 version. Research Information Database DB084, Geological Survey of Japan, National Institute of Advanced Industrial Science and Technology, https://gbank.gsj.jp/seamless/3d/index.html (Last accessed on Feb. 5, 2014).

GSI (Geospatial Survey Institute, Japan), Crustal deformation observed by synthetic aperture radar (SAR), http://www.gsi.go.jp/cais/topic110425-index.html (Last accessed on Feb. 5, 2014).

Hasegawa, S., Dahal, R. K., Nishimura, K. and Nonomura, A. and Yamanaka, M. (2009): DEM-Based Analysis of Earthquake-Induced Shallow Landslide Susceptibility, Geotechnical and geological Engineering, Vol. 27, No. 3, pp. 419-430.

Hasi, B., Ishii, Y., Maruyama, K., Terada, H., Suzuki, S. and Nakamura, A. (2011): Distribution and scale of landslides induced by recent strong reverse-fault earthquakes in Japan, Journal of the Japan Landslide Society, Vol. 48, No. 1, pp. 23-38 (In Japanese with English abstract).

Hikima, K., Miyazaki, S. and Koketsu, K. (2008): Rupture process of the 2008 Iwate-Miyagi Nairiku earthquake (Mj7.2), Japan, inferred from strong motion and geodetic data, Eos Trans. AGU, 89, No. 53, Fall Meet.Suppl., Abstract S51D1789.

Hikima, K. (2012): Rupture Process of the April 11, 2011 Fukushima Hamadori Earthquake (Mj 7.0) Two Fault Planes Inferred from Strong Motion and Relocated Aftershocks, Zisin, Vol.64, pp.243-256.

JMA (2011): About the Tohoku Pacific Ocean region, Press release No. 35 (in Japanese).

(http://www.jma.go.jp/jma/press/1104/11b/kaisetsu201104111820.pdf) (Last accessed on Feb. 5, 2014).

JMA (2012): Report on the 2011 off the Pacific coast of Tohoku earthquake, Technical Report of the Japan Meteorological Agency, No. 133, 479 p. (http://www.jma.go.jp/jma/kishou/books/gizyutu/133/ALL.pdf). (Last accessed on Feb. 5, 2014).

Kubota, T. (2002): Slope failures and landslides with Western Tottori earthquake on October 6th in 2000. Journal of the Japan Landslide Society, Vol. 38, No. 4, pp. 352-357 (In Japanese with English abstract).

McGarr, A. (1984): Scaling of ground motion parameters, state of stress, and focal depth, Vol. 89, No. B8, pp. 6969–6979.

Oglesby, D. D., Archuleta, R. J. And Nielsen, S. B. (1998): Earthquakes on dipping faults: the effects of broken symmetry, Science, 280, pp.1055–1059.

NEID (National Research Institute for Earth Science and Disaster Prevention, (2014): http://www.kyoshin.bosai.go.jp/kyoshin/quake/index_en.html (Last accessed on Feb. 5, 2014).

Shi, B. P., Brune, J. N., Zeng, Y. H. and Anooshehpoor, A. (2003): Dynamics of earthquake normal faulting: Two-dimensional lattice particle model, Bull. Seis. Soc. of America, Vol.93, No.3, pp.1179-1197.

Tainosho, Y. and Fujita, T. (1996): Mountain slope failures in the Rokko Mountains caused by 1995 HyogoKen-Nanbu earthquake - The search for teaching material development about Hyogoken-Nanbu earthquake on earth science education. Education of Earth Science, Vol.49, No.5, pp.19-26 (In Japanese).

Taira, A. (2001): Tectonic evolution of the Japanese island arc system. Annual review of Earth Planet Science, Vol. 29, pp.109-134.

Ushiyama, M. and Ohta, Y. (2009): Characteristics of death or missing caused by the Iwate-Miyagi Nairiku Earthquake in 2008, Journal of Natural Disaster Science, Vol.28, No. 1, pp. 59-66 (in Japanese with English abstract).

Yagi, H., Sato, T., Yamashina, S. and Yamazaki, T. (2008): Aerial photo interpretation map for 2008 Iwate-Miyagi inland earthquake. http://www.landslide-soc.org/education/report/iwate_miyagi_EQ_080728.jpg (Last accessed: May 18, 2010).